

Design and Testing of a Solar-Powered Amphibious Unmanned Aerial Vehicle for Long Term Autonomous Missions

Erin Yoo

June 2024

Abstract

This paper details development of testing processes and optimizations for a solar-powered unmanned aerial vehicle (UAV), called the Gannet, to ensure its reliability on a long distance mission from California to Hawaii. The first prototype of the Gannet has been testing for a year, but was not built to withstand harsh oceanic environments such as winds, waves, and saltwater. Primary task is to create a dual-function thrust stand that can operate in two modes: Static and Dynamic thrust testing. Static thrust of the motor will be evaluated through Cyclic Marine Testing that simulates a multi-day mission at sea to validate corrosion mitigation. Dynamic thrust testing will conduct a Wind Tunnel Test using various motor and propeller combinations. These tests will determine the reliability of the motor-propeller combination that is reported to produce 0.8 kg of thrust at a speed of 14 m/s and cruise power of 110 W. Secondary tasks include creating a new wing design and system identification of Gannet behavior floating on ocean surface. The wing design will consist of sourcing a lighter foam with greater water resistance, doing a carbon fiber wing lamination FEA study, and manufacturing the new wing through a wet layup process. System Identification requires analysing the field flight testing data to produce FFT (Fast Fourier Transform) plots. This can help characterise the Gannet's behavior on the surface of the water and create transfer functions for fine tuning take-off operations.

1 Introduction

The development of unmanned air vehicles (UAVs) has seen broad applications in various fields including industrial, governmental and commercial use. This project seeks to expand the horizons for UAVs by crafting a system that can perform autonomous oceanic missions lasting several weeks, with the specific goal of crossing the Pacific Ocean from California to Hawaii. Non-stop flying raises concerns with relying solely on battery life. The aircraft loses the level of autonomy needed for long distance mission due to the lack of a sustainable energy source. The fixed wing solar powered UAV, called the Gannet, will avoid the problem of non-stop flying by taking a novel approach. Solar cells were attached to the wings on the Gannet, which are a lighter alternative to gaining additional power, but not enough to maintain perpetual flight. So, the Gannet will land on the ocean surface throughout its mission to recharge. Being close to the ocean introduces additional problems which will be addressed through the design and testing of the second iteration of the Gannet.

Common classifications of UAVs pertaining to long flights include High Altitude Long Endurance (HALE), Low Altitude Long Endurance (LALE), and High-Altitude Pseudo-Satellite (HAPS)[1]. These UAVs have the same objective of maintaining flight throughout their entire mission. Although the Gannet will perform similar long distance missions, it will not be pursuing perpetual flight[2]. By landing on the ocean surface to recharge, the Gannet does not have to sustain energy parity and avoids the issue of creating a lightweight and aerodynamically perfect aircraft. The Gannet can be classified as an Amphibious Low Altitude Medium Endurance (ALAME) aircraft because the Gannet travels lower in the atmosphere and has a shorter flight time compared to similar long endurance mission based UAVs due to having a small wingspan and a higher payload. Challenges arise with having the aircraft land on open ocean waters which is why the Gannet must be designed and tested to endure waves, bio-fouling and corrosive seawater.

2 Background

There have been similar projects with creating LALE UAVs to go on oceanic journeys. Most notably, ETH Zurich's AtlantikSolar was the first solar powered UAV designed to cross the Atlantic Ocean [3]. With a wingspan of 5.65 m and mass of 7.36 kg, AtlantikSolar was able to cruise for 12 hours 22 minutes with the solar panels disengaged to replicate night time [4]. Similarly, Sky-Salor with wingspan of 3.2 m and mass of 2.444 kg made a continuous flight of more than 27 hours [5]. These examples demonstrate the feasibility of creating an UAV that can traverse the ocean. The Gannet, however, is a smaller aircraft with a 1.8 m wingspan and a heavier payload of 6.0 kg. A smaller wingspan limits the amount of solar panels that can be installed and a heavier payload decreases the flight time. Smaller scaled UAVs are unable to rely solely on solar panels for continuous flights [3] and landing is necessary to replenish energy sources before resuming flight [6].

AtlantikSolar's approach to operating is to continue its mission all night until the next morning. This strategy solves perpetual flight by staying afloat the entire time and being energy efficient. However, its key limitation is that it must only operate in sunny conditions when the sun is not too low and if the weather is not too cloudy. Gannet has roughly the same mass as the AtlantikSolar, but cannot not achieve the same strategy due to a smaller wingspan. Instead, the Gannet will take advantage of landing on the ocean surface throughout the day to recharge and land at night to sleep. A benefit of discontinuous flight is that reaching energy parity or better is not necessary and can be below budget for flight, with the solar array still assisting. Continuous daytime flying like the AtlantikSolar would be difficult to achieve since the Gannet is too inefficient. UAVs that fly lower in the atmosphere are faced with environmental challenges [7] such as clouds which can cause shading on the solar cells and exposure to salt spray. Since the Gannet will be landing on the ocean surface, it is exposed to additional environmental threats like saltwater exposure, biofouling and strong waves. To weatherproof and utilise energy conservatively, component selection and testing is essential in the Gannet's survival and performance under maritime conditions.

3 Methods

Component selection, testing and system identification can help evaluate the Gannet's ability to withstand harsh environmental conditions. The first proto-

type of the Gannet has already been created and tested in only freshwater, meaning that the Gannet has never experienced an electrolyte solution that accelerates the corrosion process of the hardware. Based on the freshwater testing, the main issues were water retention in the right wing, increased payload than originally planned, and some corroded hardware. With corrosion being one of the issues from freshwater testing, material and component selection along with testing will progress the development of a saltwater operational aircraft. The primary focus of this project was sourcing brushless motors, propellers, and electronic speed controllers (ESCs). Then these components were tested for reliability and environmental endurance. One of the secondary tasks was to source new foam for the Gannet's wings and determine how the foam deforms with and without the use of a carbon fiber laminate. In addition, system identification of the floating Gannet across various wind and wave conditions can help estimate and predict the motion of the aircraft from its prior and current behavior on the ocean surface. This is crucial to fine tuning the controls for take off.

3.1 Issues and Requirements

Field flight testing with the first Gannet has revealed the right wing soaking up more water causing forward flight to be difficult due to wing imbalance. The water eventually drains out, but the additional time and energy spent on taking off is not efficient. The first prototype of the Gannet's wings used expanded polystyrene (EPS) which is a low density foam with a measured maximum water absorption volume of 4%. Although water retention seems minimal, the added mass proved to make take off more of a challenge. To reduce water absorption in the wings, another low density foam, extruded polystyrene (XPS) was sourced to conduct a water soak test. The water soak test consists of having both foams submerged under water for 24 hours and then weighing the samples. XPS foams were measured to have a maximum water absorption volume of less than 0.5%. The Water Soak Test revealed that XPS retained less water, but slightly more dense compared to the EPS foam. XPS is 150% the mass of EPS, so mass optimization through removing material will be explored. Carving out foam and creating drainage holes could help maximize the low water absorption of XPS by reducing the total mass of the foam used. Another method of dealing with water retention is to cover the top surface of the foam wings with carbon fiber through wet lay manufacturing. The carbon fiber laminate will provide additional waterproofing and add more

structural support to the wings.

Brushless motor selection and testing is integral to the Gannet's flight performance. The first aerodynamic model of the Gannet, with a mass of 3.9 kg, yielded an estimate of 80 W for aircraft cruise. However, adjusting to the current total mass of 6.1 kg and accounting for 10% power loss to the powertrain, the expected cruise power is 165 W. Due to the current wing size and solar array configuration, the Gannet can produce 98 W in ideal weather conditions. This means that the Gannet can achieve non-stop flying if cruise power can be reduced below 100 W. To optimize the flight performance of the first Gannet, the goal is to find a brushless motor and folding propeller combination that operates at or below 200 W and take advantage of landing when energy is too low or when it is night time. Once the cruiser motor has been selected, all the motors on the Gannet will be waterproofed. The steel bearings of the motors will be replaced with ceramic bearings as those are more corrosion resistant. In addition to changing the bearings, corrosion resistant coating must be applied to the stator windings and magnets to prevent saltwater from degrading the parts inside of the motor.

The brushless motors and electrical components found on the first Gannet are either outdated or not suitable for saltwater applications and must be replaced. An online calculator, eCalc, was used to simulate and evaluate brushless motors, to help select motors along with the requirements listed below.

Brushless Motor, ESC, Folding Propeller Selection Criteria:

1. Operation at 6s (25.2 V).
2. Drives folding propeller at operating point of 14 m/s and 0.8 kg force.
3. Waterproof against seawater and salt spray.
4. Total combined mass of motor, prop and ESC below 200 g if possible.
5. ESC is DSHOT150 compatible.

Once the motors were chosen, thrust tests can help verify the results from eCalc and evaluate the Gannet's system reliability. System reliability is defined by the Gannet's consistent ability to take off and land at least once each day and endure hundreds of hours of flight time. The Gannet's performance will be evaluated through motor endurance testing and wind tunnel testing. The motor endurance testing determines the reliability of the motor by allowing the motors to run continuously while occasionally dipping into a saltwater tank to mimic the conditions

of the mission. This will be a static thrust test. Wind tunnel testing, conducted on top of a car, measures the dynamic thrust of the motor at a speed of 14 m/s. For both motor testings, a Thrust Test Stand will be designed to accommodate all the motors on the Gannet. More details pertaining to testing requirements are found below.

Thrust Test Stand and Testing Requirements:

1. Mounts motors between 19 mm and 25 mm mounting cross pattern.
2. Supports largest carbon prop size of 15-17 inches.
3. Sustains a maximum force of over 5 kg.
4. Reliability Testing with thrust test runs of 24, 48 or 72 hours, with 12 hour intervals of rest while soaked in solution, and multiple dunking events between runs during thrust testing.
5. Measurements should be accurate to 20 g and have good repeatability.
6. Measured with a bandwidth (or sample rate) on the order of 10 Hz, perhaps up to 100 Hz.
7. Can ramp the motors from 0 to 100% duty cycle in about 4 or 5 seconds and have around 200 to 1000 thrust setpoints asserted in that ramp. For the test at 14 m/s on the top of the car, the thrust setpoint will likely be around 85%.
8. Cushioning where it interfaces with the car roof rack such that bumps in the road don't couple to the strain gauge measurement.
9. Support the motor up to a meter above the roof rack.
10. Stand must be compliant with saltwater testing.

System identification of the floating Gannet will provide a mathematical model that can predict the output given a wave input. If the Gannet was floating on the ocean surface and started to encounter rough waves, the aircraft should be able to take off at the exact moment it is at the top of a wave. Currently, the Gannet does not have a response system to harsh waves which is why it is important to start with establishing a baseline of the Gannet floating in normal wave conditions. Characterizing the Gannet behaviors under different wave conditions can help develop a better control model for take off.

3.2 Wing Design and Testing Process

To compare the material properties of EPS foam a potential substitute, another pair of Gannet wings were cut from XPS foam using a bow-tensioned hot wire. The XPS foam wings were cut based on the measurements and jigs for the first Gannet's wings. Two alligator clips were attached to opposite ends of the wire and then connected to a DC power supply with a setting of 25 volts and 2 amps. This heated only the metal wire in between the alligator clips, allowing it to easily cut through foam. The jigs provided a guide line for the hot wire to follow and cut out the curvature needed for the wings. Along with creating a new wing prototype to test and get real world data, Finite Element Analysis (FEA) was used to compare the amount of deflection that occurred for EPS and XPS with the same force applied to the wings.

3.3 Thrust Test Stand Design Process

The Thrust Test Stand was conceptualised using CAD to ensure there were proper degrees of freedom as well as constraints to keep the stand in its desired position. The main requirement was that the test stand could allow the motor to lower itself into the test tank, but go back to an upright position. Stronger material, such as aluminium and carbon steel, were selected for the manufacturing process as opposed to 3D printing the parts. Since the stand would also be exposed to the saltwater during testing, non-corrosive metals were chosen. The entire assembly of the Thrust Test Stand can be seen in Figure 1.

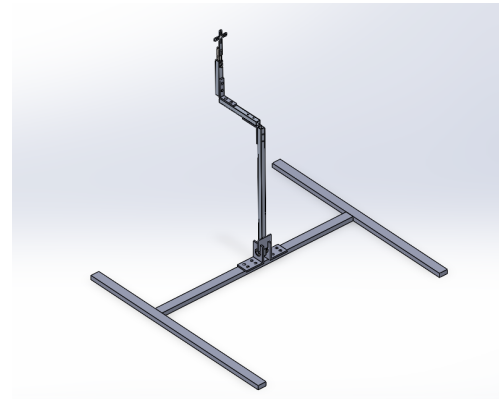


Figure 1: Complete assembly of the Thrust Test Stand made in Solidworks.

FEA was used to validate the design of the motor mount by ensuring it can withstand up to 5 kg of force

from the motor. Due to limited materials, the motor mount was made from an aluminium plate with 0.125 inch thickness. The FEA results, Figure 2, for this material showed a maximum deflection of 10.06 mm. The force in the FEA was modelled with the direction pointing out the mount because the thrust generated from the propellers would pull the motor forward. There is maximum deflection of 1.61 mm for 0.8 kg of thrust which force required for cruise speed.

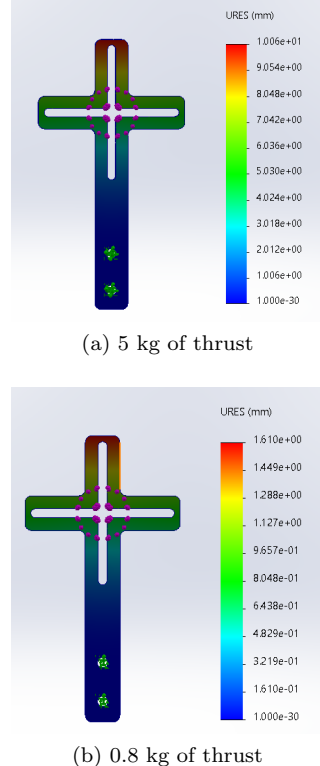


Figure 2: Solidworks FEA of 0.125 inch thick Motor Mount

Detailed features of the thrust stand can be seen in Figure 3. The Z-Bar configuration accommodates for the lip of the test tank to allow the motor to submerge up to 10 cm. At the bottom of the Z-Bar, there is a press fit carbon steel shaft that goes through the bar, rigidly constraining it. This shaft with the Z-Bar is placed in between two 90° angle brackets at the base of the stand. The 90° angle brackets has press fit bearings allowing forward and backward rotation of the Z-Bar. A hardstop was placed into the front of the stand, press fit between the two angle brackets and into the slots, to prevent only allow a 90° of the stand during Cyclic Marine Testing. The hardstop also constrained the distance between the two angle brackets, ensuring both ends of the shaft stick out on the other side of the brackets. For the wind tunnel

testing, an additional hardstop will be placed on the slots of the angle brackets to constrain all degrees of motion of the test stand. A closer look at the hardstop and angle bracket configuration can be seen in Figure 3a. Thrust measurements will be taken from a single point load cell , shown in Figure 3b, where the bottom of the motor mount is connected to the top load cell and the bottom of the load cell is secured to the Z-Bar.

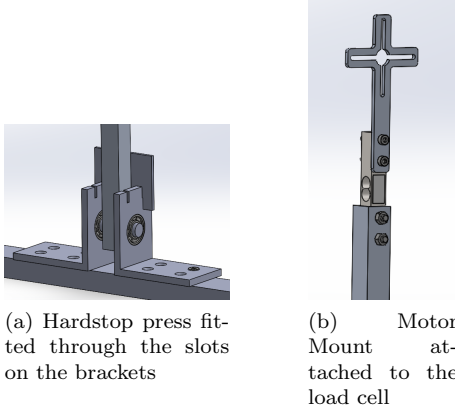


Figure 3: Components of the Thrust Test Stand

The thrust tests logged the following data below and saved it to a csv file in a python script using ROS and MAVROS. Wind Tunnel Testing have additional data numbers 6-8.

Data logged:

1. Time elasped in testing (s)
2. Thrust measurement (kg)
3. Battery Voltage (V)
4. Battery Current (A)
5. Throttle (Pulse width modulation - PWM)
6. Air speed (m/s)
7. Ground speed (m/s)
8. ESC RPM (1/min)

The load cell measurements were obtained by connecting it through the four spring terminal on the NAU7802 which is a load cell amplifier that helps interpret the weak output signals. NAU7802 was then connected to the Edge2 IO Module using the I2C pins. The IO Module allowed the load cell to communicate to a Small Board Computer (SBC), Khadas Edge2, that was responsible for running the test scripts. Figure 4 displays the hardware setup to

test the communication between the NAU7802 amplifier and Edge2. The two probes of the oscilloscope were connected to the ground wire of the IO module which captured signals sent and received between serial data (SDA) and serial clock (SCL). After establishing a connection between Edge2 and the load cell, the three SDC outputs were converted into one signed integer output using the functions from the NAU7802 Python Library. This signed integer value would be the thrust force measurements.

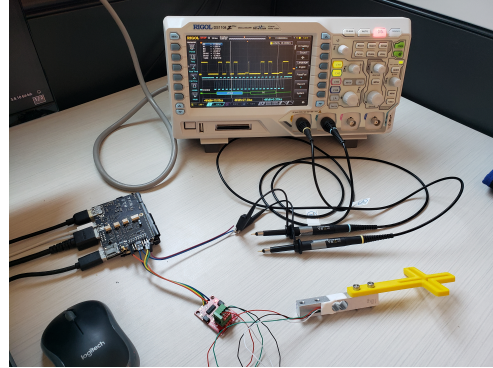


Figure 4: Components from left to right: Edge 2 with IO module attached, NAU7802, load cell with the motor mount, and an oscilloscope with two probes.

To validate thrust measurements, the load cell was calibrated using an object and digital scale. The load cell was secured onto the test stand and the object was placed onto the motor mount. The 3D printed motor mount in Figure 4 was not used for the calibration process and instead the CNC milled aluminium mount was used. The calibration process, seen in Figure 5, was repeated 20 times. The python script outputted the calibration factor and thrust measurement readings each time. The 20 calibrations factors were recorded and the mean value from the Gaussian Distribution was used to set the calibration factor.



(a) Step 1: Make sure nothing is on the mount and start script.



(b) Step 2: Weigh object.



(c) Step 3: Put object on the mount.

```
Put known mass on load cell
Mass in kg: 0.423
Calibration factor: -105594.77541371158
Thrust: 0.4222
Thrust: 0.4198
Thrust: 0.4216
Thrust: 0.4236
Thrust: 0.4215
Thrust: 0.4230
Thrust: 0.4229
Thrust: 0.4227
Thrust: 0.4216
Thrust: 0.4233
```

(d) Step 4: Verify thrust readings

Figure 5: Calibration Process

An important aspect of the hardware setup was to use a shielded cable to minimize any external noise and electromagnetic interference (EMI) from the environment. This was deemed necessary after installing the load cell onto the test stand and discovering that the load cell no longer reacted accordingly with applied force. The thrust measurements were inconsistent and did not match the expected force applied. The NAU7802 amplifier board was discovered to be susceptible to any electromagnetic fields produced by any object or movement near it, which impacted the thrust readings. Figure 6 is the wiring diagram used to solder the load cell onto one end of the shielded cable and the load cell amplifier board onto the other end. The shielded cable was then fed through the square tubes on the Thrust Test Stand for a cleaner assembly and out of the way of the propellers.

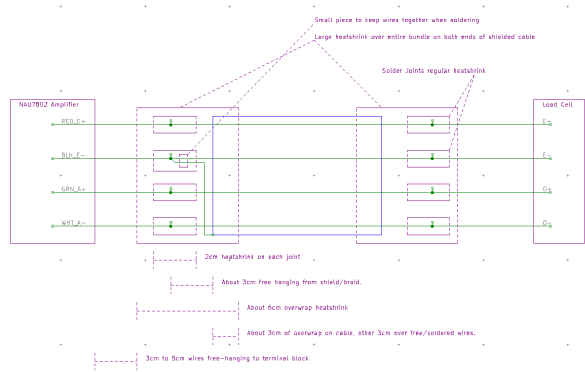


Figure 6: Wiring and Solder Diagram to connect 1 meter long shielded wire to the load cell and NAU7802 amplifier board. The BLK_E- wire on the NAU7802 amplifier has an additional wire, drain wire, from the shielded cable soldered. This serves as the ground connection for the shield.

3.4 Motor Thrust Testing Process

Wind Tunnel Testing was conducted by latching the Thrust Test Stand on top of a car using ratchet straps. The setup along with the attached pitot tube can be seen in Figure 7. The test stand was about 1 meter high to reduce the car's aerodynamic influence on the motor. Wind Tunnel Testing logged the same data as the Cyclic Marine Testing, but also included air speed and ground speed from the pitot tube to help analyse the dynamic thrust results. The test script did not include ramping the motors up and down through MAVROS motor commands. The remote controller was used to manually change the throttle to easily cover all PWM values at different air speeds. The car speed was mostly around the Gannet's cruise speed of 14 m/s with slight fluctuations to set the motor's endurance across a variety of air speeds.



Figure 7: Wind Tunnel Testing Setup. Wooden planks were strapped to the railing on the car roof.

The script for Cyclic Marine Testing has been completed, but not tested. This section outlines the set up procedure to run the test. A large plastic pool with saltwater mix should be prepared to imitate the corrosive nature of ocean water. Then, the Thrust Test Stand should be placed at the same height of the pool. To ensure accurate and repeatable measurements, the load cell specifications must be checked to ensure there would be a small total error percentage. The hardstop at the back of the Z-Bar, the side where the bar sticks outward, will be removed to allow for a full 90° rotation. Once the testing site is prepared, the test script will be commanded to run on the Edge 2 which will be connected to the test stand as seen with the Wind Tunnel Testing. The test script was an open-loop process that followed the sequence below:

1. Arm the autopilot
2. Every 200ms, increment the motor output by 5%, until it has reached 100%, and continue to issue the motor output commands every 200ms at 100%
3. Continue for 60 seconds
4. At the end of the run timer, decrement the motor setpoint by 10% each interval
5. Once the motor output has decremented to 0%, the 200ms inner loop that updates the motor output can be exited, but have the script wait about 5 seconds before the next action.
6. Disarm the autopilot
7. Wait 60 seconds. This simulates a rest interval on the ocean surfaces. When the motor relaxes, it should drop to the bucket/pool surface.

Cyclic Marine Testing will start off by having the motor rest in the pool. Once the test script runs, the motor will turn on and the thrust generated from the propellers will raise the stand out of the pool. The hardstop will stop the stand once it reaches an upright position. Then, the motor will disengage and fall into a pool of salt water which will test corrosion and water resistance. This process will repeat while logging data of the motor thrust force from the load cell and information about battery voltage and current at the elapsed time.

3.5 System Identification Process

System identification of the floating Gannet with the motor disengaged can help estimate and predict the motion of the aircraft from its prior behavior on the ocean surface. The yaw, roll and pitch data from the first Gannet's flight test was cross referenced with the video footage to determine the time frame where the aircraft's system was encountered with little to no waves. The data of the floating aircraft on calm waters was extracted to create a Fast Fourier Transform (FFT) plots.

4 Results

4.1 FEA of the Wing

FEA was set up so that the root of the Gannet's right wing was fixed with 1 kg (9.81 N) of force was applied perpendicular to the top surface. Also, the one ply of carbon fiber was modelled with 0.6 mm thickness. The FEA results of the wing revealed that having one layer of a carbon fiber laminate on the top surface significantly reduces deformation. From Figure 8a, the highest deformation for the EPS foam wing without carbon fiber was 41.04 mm and Figure 8b shows that with carbon fiber the highest deformation is 4.95 mm. FEA demonstrates that having carbon fiber adds additional stiffness to the foam board, decreasing deformation at most tenfold.

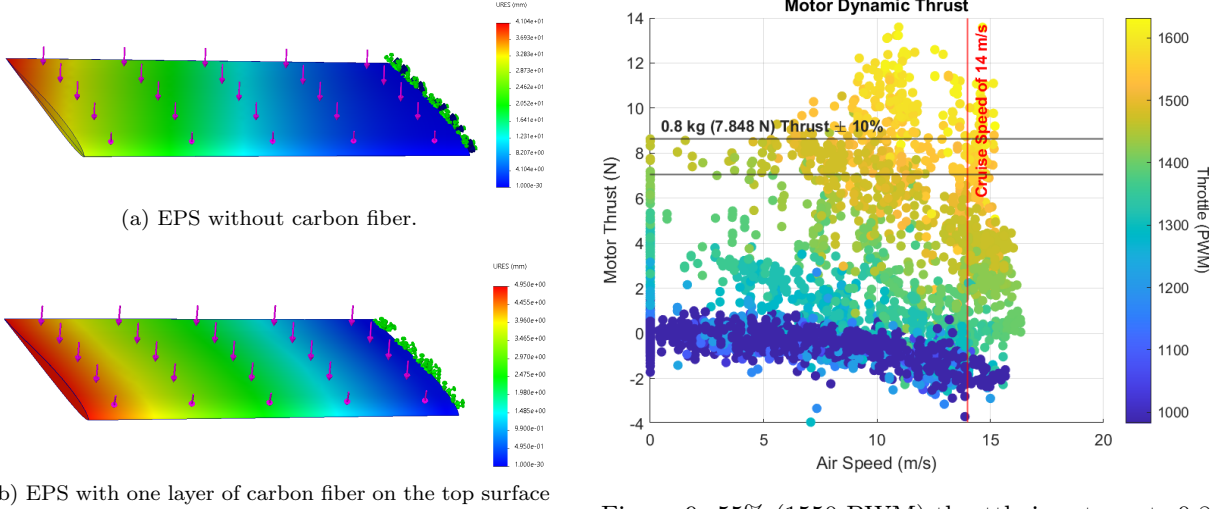


Figure 8: FEA on EPS Rigid Foam

The FEA results for the XPS foam wing revealed a maximum deformation of 49.35 mm without the carbon fiber and 1.896 mm with the carbon fiber. The displacement images for the XPS FEA were not shown because of the similarity to the EPS FEA images.

4.2 Dynamic Thrust of the Cruiser Motor

Dynamic thrust is impacted by airspeed which was why the pitot tube was attached to the stand in order to get those measurements. Dynamic thrust produced by the motor can be visualised in Figure 9 where the relationship between motor thrust force, air speed and throttle values are found. As the throttle inputs increase at 14 m/s, the amount of thrust produced increases as well. To fall within 10% of the required thrust force to cruise at 14 m/s, the Gannet must be operating at a minimum of 50% throttle input or 1500 PWM.

Towards the end of testing, the motor mount seemed to have bent slightly forward due to thrust generated by propellers. FEA results show that the mount will deform noticeably with 5 kg of thrust, but was bent with at most 1.42 kg of force (largest thrust value from data collected). Having a bent motor mount may have had an impact on the load cell taking the thrust measurements.

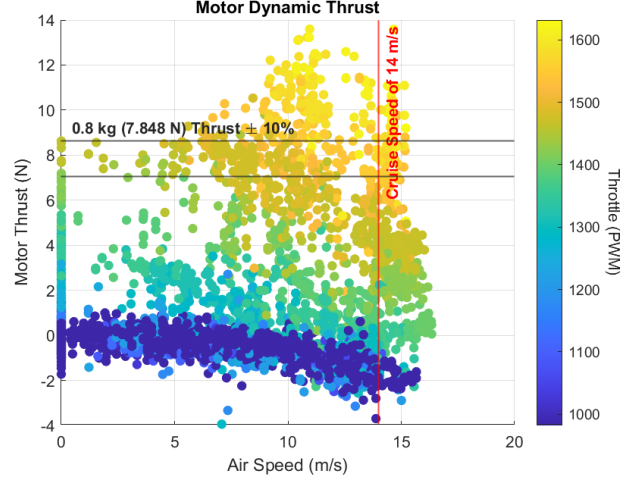


Figure 9: 55% (1550 PWM) throttle input meets 0.8 kg thrust needed to cruise at 14 m/s.

The amount of power produced from the motor was calculated by multiplying the thrust produced by the propellers by the air speed reported by the pitot tube. Figure 10 shows the plot of motor thrust against the throttle inputs to visualise how the mechanical power out of the system compares to varying throttle inputs.

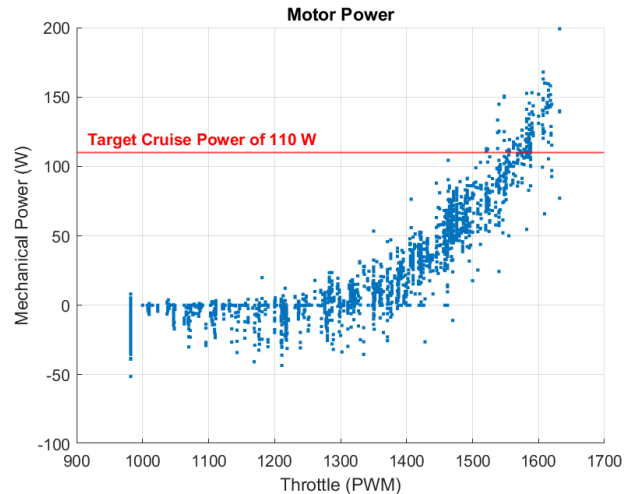


Figure 10: As expected, there is an upwards trend where mechanical power increases as the throttle input increases. Target Cruise Power = $0.8 \text{ kg} \times 14 \text{ m/s} \times 9.81 \text{ m/s}^2 \approx 110 \text{ W}$.

Efficiency of the system was calculated by dividing mechanical power out by the electrical power in. Electrical power into the system was found by multiplying the voltage by the current supplied to the motor. In the logged data file, the values for current were negative, indicating that the wiring was

switched. The current was assumed to be positive to create Figure 11. The linear regression model of the data shows that there is 37.87% efficiency for the current mechanical and electrical system. This is lower than the expected efficiency value of 70% and the loss of power to the motor must be investigated. Further testing can help determine if there were any discrepancies within the data collected.

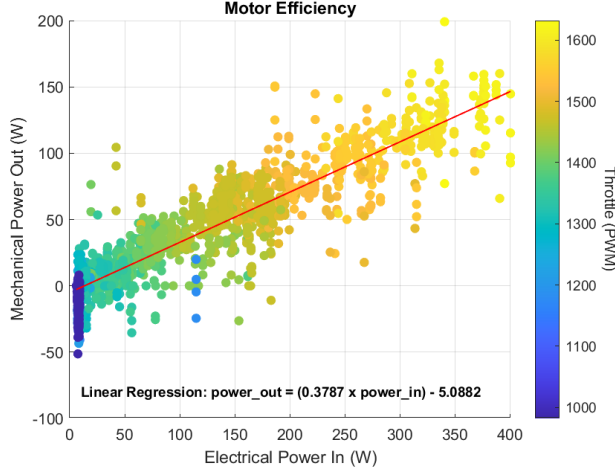


Figure 11: The mean Efficiency (η), or $\text{power_out}/\text{power_in}$, across all PWM values is 0.3787 (trend line slope).

4.3 System Identification of the Gannet's Pitch

The FFT plot for the pitch will be discussed because the up and down motion of the aircraft's nose is the most prevalent mode of bobbing on the surface. This can be used to time exactly when the Gannet would need an automated take off. The Gannet's pitch was characterised by looking at an input wave frequency from 0 to 5 Hz. Figure 12 shows the maximum peak magnitude which is the most common frequency of the aircraft's pitch during that segment of the data.

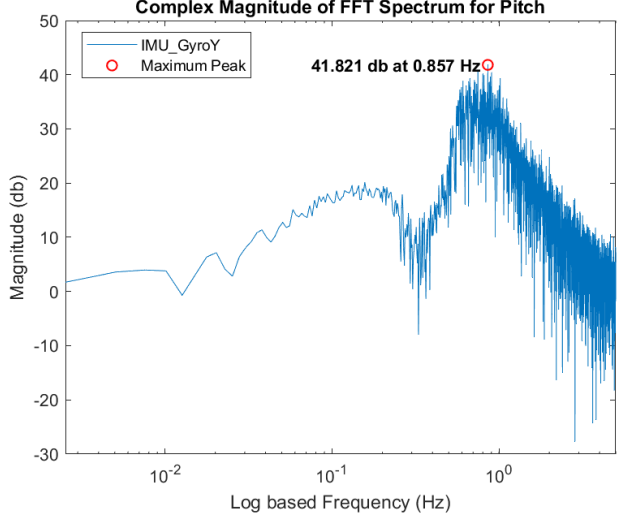


Figure 12: FFT Plot of the Gannet's Pitch during a 10 minute time frame where it was floating in Silver Lake. The maximum peak is found at 0.857 Hz with a magnitude of 41.821 db.

5 Conclusions

The second prototype of the wings will use XPS foam due to less deformation, and more favorable waterproofing. Carbon fiber will not be used although it significantly reduces deformation. One ply weighs little less than 0.5 kg, so the total mass of 1 kg added to the aircraft would cause more difficulty during take off.

Wind Tunnel Testing evaluated the motor performance under dynamic thrust by measuring the thrust under various air speeds and throttle inputs. For the Gannet to maintain cruise speed, the motors must be set at least 1550 PWM. Testing should be repeated multiple times, but with a thicker motor mount to withstand bending moment generated by the thrust.

5.1 Future Work

The use of carbon fiber adds stiffness to the wings reducing the total amount of deflection that can occur. This can be really useful for long term autonomous missions and should be further explored. The extra mass added to the Gannet when adding carbon fiber was the sole issue of deciding to not use the composite and this can be solved through carving out sections of the wing. Reducing the mass of the wing by making drainage holes and then adding carbon fiber could be another wing prototype. Multiple water soak tests for both the EPS and XPS foams can be done to determine if water retention is uniform throughout or

if there are certain areas that are more likely to hold water. Areas that retain more water repeatedly could be carved out for the water to drain out faster. FEA analysis can also be run on this new wing to compare deformation results with the the results of the current wing. In addition, Computational Fluid Dynamics (CFD) simulation can be ran to determine if creating drainage holes will impede the aerodynamic structure of the wings.

Cyclic Marine Testing has to be conducted to collect data for static thrust. Currently, the motor commands sent to the Gannet through ROS is not executing and must be addressed to ensure the Thrust Test Stand can reliably dunk the motor in and out of the test tank over 24 hours. Both the Cyclic Marine and Wind Tunnel Testing should be repeated multiple times to collect more data and reduce any discrepancies from the readings and test set ups. Once this has been done for all the motors on the Gannet, the bearings of the motors will be replaced by ceramic bearings and the two thrust tests will be repeated. Motor performance of the ceramic bearings will be evaluated and compared to the normal steel bearings.

Since the FFT of yaw, roll, and pitch have been found, transfer functions must be derived to model the Gannet's system. The transfer function would be able to predict the output, how the Gannet will react, when given the input, size and speed on the wave on the ocean surface.

6 Acknowledgement

This material is based upon work supported by the National Science Foundation under Grant No. IIS-2150394. Any opinions, findings, and conclusions or recommendations expressed in this material are those of the author(s) and do not necessarily reflect the views of the National Science Foundation.

Robotic Workers Lab at the University of Nevada, Reno

References

- [1] Adam C Watts, Vincent G Ambrosia, and Everett A Hinkley. "Unmanned aircraft systems in remote sensing and scientific research: Classification and considerations of use". In: *Remote sensing* 4.6 (2012), pp. 1671–1692.
- [2] Stephen J Carlson et al. "The Gannet Solar-VTOL: An Amphibious Migratory UAV for Long-Term Autonomous Missions". In: *2023 International Conference on Unmanned Aircraft Systems (ICUAS)*. IEEE. 2023, pp. 419–424.
- [3] Andre Noth. "Design of solar powered airplanes for continous flight". PhD thesis. ETH Zurich, 2008.
- [4] Philipp Oettershagen et al. "A solar-powered hand-launchable UAV for low-altitude multi-day continuous flight". In: *2015 IEEE international conference on robotics and automation (ICRA)*. IEEE. 2015, pp. 3986–3993.
- [5] Luis Miguel Almodôvar Parada. "Conceptual and preliminary design of a long endurance electric UAV". In: *PhD diss., Master's thesis, Instituto Superior Técnico, Universidade de Lisboa* (2016).
- [6] Richard-Alexandre Peloquin, Dominik Thibault, and Alexis Lussier Desbiens. "Design of a passive vertical takeoff and landing aquatic UAV". In: *IEEE Robotics and Automation Letters* 2.2 (2016), pp. 381–388.
- [7] Perry J Hardin and Ryan R Jensen. "Small-scale unmanned aerial vehicles in environmental remote sensing: Challenges and opportunities". In: *GIScience & Remote Sensing* 48.1 (2011), pp. 99–111.